Wind-induced cross-strait sea level variability in the Strait of Gibraltar from coastal altimetry and in-situ measurements

J. Gómez-Enri[a*], C.J. González[a], M. Passaro[b], S. Vignudelli[c], O. Álvarez[a], P. Cipollini[d], R. Mañanes[a], M. Bruno[a], M. P. López-Carmona[e], A. Izquierdo[a].

[a] Applied Physics Department (University of Cadiz). Puerto Real (Cadiz), 11130, Spain.
[b] Deutsches Geodätisches Forschungsinstitut der Technischen Universität München (DGFI-TUM), Munich, Germany.
[c] CNR Institute of Biophysics (CNR-IBF), Pisa, 56024, Italy.
[d] Telespazio Vega for ESA Climate Office, Harwell, United Kingdom.
[e] Spanish Meteorological Agency (AEMET), Rota, Spain.

* Corresponding author: jesus.gomez@uca.es

Abstract

Coastal altimetry products are available and are being extensively validated. Their accuracy has been assessed in many coastal zones around the world and they are ready for exploitation near the shore. This opens a variety of applications of the sea level data obtained from the specific reprocessing of radar altimeter signals in the coastal strip. In this work, we retracked altimeter waveforms of the European Space Agency satellites: ERS-2 RA and Envisat RA-2 from descending track (#0360) over the eastern side of the Strait of Gibraltar using the Adaptive Leading Edge Sub-waveform (ALES) retracker. We estimated along-track Sea Level Anomaly (AT_SLA) profiles (RA-2) at high posting rate (18 Hz) using improved range and geophysical corrections. Tides were removed with a global model (DTU10) that displays a good performance in the study area: the mean root square sum (*RSS*) of the main constituents obtained with *DTU10* and 11 tide gauge stations was 4.3 cm in agreement with the *RSS* using a high-resolution local hydrodynamic model (*UCA2.5D*) (4.2 cm). We also estimated a local mean sea surface by reprocessing ERS-2/Envisat waveforms (track #0360) with ALES. The use of this local model gave more realistic AT_SLA than the values obtained with the global model DTU15MSS. Finally, the along-track Absolute Dynamic Topography (AT_ADT) was estimated using a local Mean Dynamic Topography obtained with the local hydrodynamic model UCA2.5D. We analysed the cross-strait variability of the sea level difference between the African / Spanish coasts along the selected track segment. This was compared to the sea level cross-strait difference from the records of two tide gauges located in the African (Ceuta) and Spanish (Tarifa) coasts. The sea level differences from altimetry and tide gauges were linked to the zonal component of the wind. We found a positive and significant (>95% c.l.) correlation between easterlies / westerlies and positive / negative cross-strait sea level differences between the southern and northern coasts of the Strait in both datasets (altimetry: r = 0.54 and in-situ: r = 0.82).

Keywords: Strait of Gibraltar, cross-strait sea level, satellite altimetry, tide gauge, wind-induced.

1. Introduction

Sea level is one of the Essential Climate Variables (ECV) listed in the Global Climate Observing System inventory (GCOS, 2016). The European Space Agency (ESA) launched in 2010 the Climate Change Initiative (CCI), aiming at providing the most accurate and homogeneous time series of some ECVs for climate studies, including altimeter-derived sea level records, such as gridded monthly maps of Sea Level Anomaly (SLA) (Quartly et al., 2017; Legeais et al., 2018) (http://www.esa-sealevel-cci.org/). Despite all the benefits of using gridded altimetry products in many applications (e.g., scientific, social, commercial), their use is more problematic in coastal zones due to poor spatio-temporal resolution of the products and processing difficulties (Vignudelli et al., 2011). These difficulties have been mitigated thanks to the efforts made in the last decade by the coastal altimetry community (http://www.coastalt.eu/community). Basically, the success is based on the generation of accurate along-track altimetry products near the shore (see Vignudelli et al. (2011); Cipollini et al. (2017); and references therein).

In recent years, many works are found in the literature focused on the generation and validation of improved along-track 'coastal' datasets from past to present altimetry missions. All of them are based on the analysis of improved geophysical corrections to the altimeter *Range* (Brown, 2010; Carrère and Lyard, 2003; Handoko et al., 2017; among others), and/or more dedicated retracking processing which take into account the shape of the radar waveforms near the coast (basically, due to land or calm water contamination) (Gommenginger et al., 2011; Passaro et al. 2014; Peng and Deng, 2018; Röscher et al., 2017). A summary table with all the datasets available to date for coastal altimetry can be found in Cipollini et al. (2017). There is no operational coastal altimetry product available yet, however, the experimental data sets that are already validated can now support the investigation of specific ocean processes occurring in regions close to land. The available experimental datasets offering retracked Ranges are the Adaptive Leading Edge Sub-waveform ALES (from the Physical Oceanography Distributed Active Archive Center-PODAAC and from the Open Altimeter Database-OpenADB (https://openadb.dgfi.tum.de/en/data_access/; Passaro et al., 2014) and Prototype Innovant de Systèm de Traitement pour les Applications Côtières et l'Hydrologie-PISTACH (CNES) (https://www.aviso.altimetry.fr/en/data/products/sea-surface-height-products/global/coastal-and-hydrological-products.html; Mercier et al., 2010). In a recent work, Xi-Yu et al. (2018) used a parameter available in the Jason-2 Geophysical Data Record and considered a coastal band of up to 70 km in their analysis offshore Hong Kong. Notably, the work was an independent study that compared ALES data against data from the PISTACH coastal retracker and rated the first as the one giving the best results, while pointing out that a careful outlier analysis was needed.

Despite all these efforts, little is still done in the use of along-track high-resolution products (from 18 Hz to 80 Hz, corresponding to along-track distance between two consecutive measurements from ~350 m to ~85 m) for oceanographic applications in the coastal strip. Exploitation of such products is crucial for many applications (infrastructure designs, coastal zone protection, and improvements in ship route security, among others) and to characterise the different processes (coastal sea level change, storm surges, coastal currents and fronts, etc.) observed in the coast. Improved reprocessing of along-track coastal altimetry data is important for coastal observing systems (monitoring) and to re-analyse previous datasets. Recently, Dong et al. (2018) identified tidal mixing fronts using Jason-2 20-Hz along-track SLA data over

Georges Bank (Northwestern Atlantic Ocean). Han et al. (2012) analysed 20-Hz and 1-Hz Jason-2 data to study Hurricane Igor storm surge off Newfoundland (Canada). At seasonal time scales, Passaro et al. (2015) determined the annual cycle of the sea level in the Baltic Sea/North Sea transition zone and Passaro et al. (2016) observed the seasonalities and trends of internal seas in the Indonesian Archipelago, using the ALES 18-Hz data set from Envisat RA-2. Here we propose to exploit the information in along-track altimetry in our study area, the Strait of Gibraltar. The product could be used to better understand and monitor the local oceanographic processes taking place in such a complex environment and to estimate transports, and therefore water exchange, contributing to 1) closing the water balance over the Mediterranean basin; 2) monitoring changes in the Mediterranean outflow under climate change conditions; and 3) monitoring the wind-induced changes in the sea level of the Mediterranean and Black seas.

The questions addressed here are of large scientific and societal impact. The Mediterranean Water outflowing the Strait of Gibraltar contributes to maintain the high salinity of the Norwegian Sea (e.g. Reid, 1979), a key area for deep water formation in the North Atlantic and, on the other side, the net flow through the Strait of Gibraltar must close the water budget over the Mediterranean basin (Candela, 2001). This is why monitoring exchange flows through the Strait of Gibraltar has been proposed as a key action for climate studies of the Mediterranean and the Global Circulation (Candela, 2001). The sea level in the Strait of Gibraltar will react to changes in the flow. Therefore, monitoring the sea level signal will provide us information on exchange flows through the Strait of Gibraltar (Hughes et al., 2015). At the same time, local wind forcing in the Strait of Gibraltar has a far reaching impact in terms of spatial and time scales. Garcia Lafuente et al. (2002) estimated that the wind forcing contribution to exchange flows through the Strait of Gibraltar is of 0.3 Sv, and Fukumori et al. (2007) suggested that altimetry observed basin-wide sea-level interannual variability in the Mediterranean Sea was linked to winds in the Strait of Gibraltar area. The driving mechanism, according to Menemenlis et al. (2007), is the Atlantic Ocean to Mediterranean Sea sea-level difference reaction to the along-strait wind set up. Calafat et al. (2012) showed that the observed tide gauge decadal variability in the Mediterranean Sea is mostly driven by mass exchange through the Strait of Gibraltar, which is also affected by local winds. The hypothesis that local wind in the Strait of Gibraltar area drives basin-wide sea-level changes in the Mediterranean Sea is further supported by sea-level altimetry and ocean mass GRACE data analysis (Landerer and Volkov, 2013). More recently Volkov and Landerer (2015) and Volkov et al. (2016) highlighted that local winds in the Strait of Gibraltar also affect the Black Sea sea level variability.

The main contribution of this work is twofold: (1) analysis of the oceanographic content of coastal altimetry products at high-spatial resolution along track (~350 m between two consecutive 18-Hz sea level measurements) in the Strait of Gibraltar; and (2) exploitation of these products for a better understanding of the oceanographic processes in the study area. To do this, we estimated along-track Absolute Dynamic Topography (ADT) profiles obtained from the European Space Agency (ESA) Envisat RA-2 descending track #0360 (Figure 1) using the coastal-dedicated ALES retracker and accurate range and geophysical corrections. We analysed their spatio-temporal variability by estimating the sea level difference between the southern and northern sectors of the track segment and its relationship with the wind regime. The present paper is a step forward in the use of accurate altimeter products to extract relevant information of oceanographic processes close to coastal zones, such as the Strait of Gibraltar.

The paper is organised with Section 2 describing the study area (Strait of Gibraltar). Section 3 gives details of the datasets and method used to estimate the Absolute Dynamic Topography. The results are presented in Section 4 and discussed in Section 5. The paper ends with the concluding remarks in Section 6.

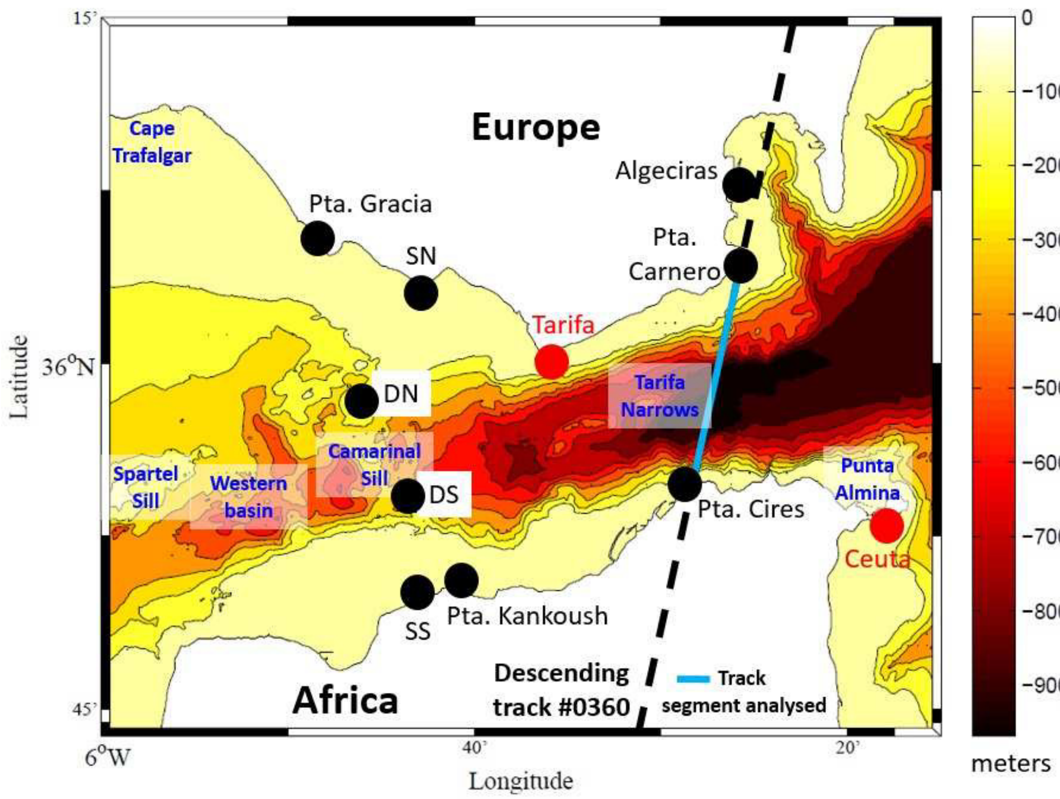

Figure 1. Study area: The Strait of Gibraltar between Europe and Africa. Colour scale indicates the bathymetry (in meters). Also shown the location of ERS-2 / Envisat descending track #0360 (the track segment analysed is highlighted in blue), the main topographic features mentioned in the text, and the location of the tide gauge and bottom pressure measurement sites used for validation of the tidal constituents. Red circles indicate the tide gauges used in the analysis of the cross-strait variability.

2. Study area: The Strait of Gibraltar

The Strait of Gibraltar is the choke point connecting the Atlantic Ocean and the Mediterranean Sea. Its bathymetry is shallower in the western part featuring the Spartel sill (depth 300 m) and the Camarinal sill (depth 280 m) separated by the Western basin. The Strait then deepens to 1100 m to the East in the Tarifa Narrows (Figure 1).

Due to the presence of less-salty, warmer Atlantic waters in the upper water masses, and saltier, cooler Mediterranean waters underneath, there is a strong density-stratification in the water column within the Strait. This leads to an inverse estuarine circulation with a two-layer exchange with a net resulting eastward flow needed to close the Mediterranean Sea water and salt balance. Lacombe and Richez (1982) characterised the hydrodynamic regime of the Strait distinguishing three main scales of variability:

(i) long period: related to seasonal, interannual, and longer period fluctuations (e.g. Garrett et al., 1990; Candela et al., 1989; Brandt et al., 2004);

(ii) subinertial: ranging from few days to few months, it is related to the exchange flows modulation caused by meteorological forcing (Candela et al., 1989). Winds are the most important meteorological forcing. Their regime is zonal with alternating easterlies-westerlies, reaching mean speeds up to 20 m s^{-1}. The alternated winds affect the along and cross-strait dynamics (Stanichny et al., 2005);

(iii) tidal, which represents the most energetic process in the Strait shows a predominant semidiurnal character but with a significant diurnal contribution. Tidal current velocities are strong enough to periodically reverse the flow in both layers near Camarinal Sill (Candela et al., 1990).

3. Datasets and methods

In this work we used accurate coastal altimetry products from the European Space Agency Satellites ERS-2 RA and Envisat RA-2 (subsection 3.1) combined with a global tidal model, a local hydrodynamic model and mean sea surface models presented in subsections 3.2 and 3.3, respectively. The experimental data (tide gauge, bathymetry and wind velocity) are described in subsection 3.4. Finally, the methodology used to estimate the along-track Absolute Dynamic Topography is explained in subsection 3.5.

3.1 ERS-2 RA and Envisat RA-2

Along-track sea surface heights and sea level anomalies (*AT_SLA*, henceforth) 18 Hz were retrieved from the track #0360 of ERS-2 RA (cycle 1 to cycle 85, from May 1995 to June 2003) and Envisat RA-2 Phase E2 (cycle 6 to cycle 93, from May 2002 to September 2010) during the 35-day repetitive orbit of the missions. ERS-2 / Envisat RA-2 track crossed the eastern side of the Strait at 11:15 / 10:46 UTC times, respectively (Figure 1). Along-track measurements for each cycle were linearly interpolated to the 18-Hz nominal locations. We followed the methods explained in Gómez-Enri et al. (2016) to obtain *AT_SLA* (Envisat RA-2) using different sources of information and fields:

- Sensor Geophysical Data Records (SGDR) official product: *orbit*, *ionospheric*, *dry / wet tropospheric*, *solid earth tide and pole tide* corrections (ESA, 2007).
- Adaptive Leading Edge Subwaveform (ALES) retracker: *range*, *sigma0* and *significant wave height* (*SWH*) (Passaro et al., 2014).

- Danmarks Tekniske Universitet (DTU): *mean sea surface* (*DTU15MSS*, Andersen et al., 2016) and *tidal model* (*DTU10*, Cheng and Andersen, 2011).

Some of the corrections available in the SGDR were at a 1-Hz along-track spatial resolution, so they had to be linearly interpolated to 18 Hz prior to application to the high-rate data. *sigma0* and *SWH* from ALES were used to re-compute the *Sea State Bias* (*SSB*) correction. Gómez-Enri et al. (2016) validated time series of *AT_SLA* for the same track segment within the Strait using the same products (with the exception of the mean sea surface as they used an older version) against *in-situ* tide gauge data. They found about a 20% of improvement with respect to the *AT_SLA* computed with the *range* and *SSB* available in the SGDR official product. This was a promising result in terms of accuracy of altimetry data in the study area.

AT_SLA profiles (18 Hz) were estimated following Eq. (1):

$$AT\_SLA = Orbit - Range - Range\ Corrections - Geophysical\ Corrections - MSS \quad (1)$$

where *Orbit*, is the distance between the satellite's orbit and the WGS84 reference ellipsoid. *Range*, is the retracked range from ALES. *Range Corrections* are: *ionospheric*, *dry / wet tropospheric*, *SSB*. The set of *Geophysical Corrections* are: *solid earth, geocentric pole* and *total geocentric* ocean tides.

3.2 Global tidal model and local hydrodynamic model

As mentioned, coastal altimetry products with a good level of accuracy and high spatial resolution along track (~350 m) are becoming available thanks to a number of free datasets (see Introduction section). Efforts are now needed in order to extract, assess and exploit the oceanographic content of the coastal altimetry products, especially in challenging zones such as the Strait of Gibraltar. The use of global tidal models in coastal zones to de-tide the satellite-derived sea level oscillations might be one of the main sources of noise in the sea level estimates and as such should be verified with care. In this paper, we assessed the constituents of a global tidal model: *DTU10* (Cheng and Andersen, 2011) and the ones obtained from a local hydrodynamic model: *UCA2.5D* (Izquierdo et al., 2001), using in-situ measurements.

3.2.1 Global tidal model DTU10

The model *DTU10* is an updated version of *FES2004* (Lyard and Lefèvre, 2006) ocean tide. Its resolution is 0.125° x 0.125° worldwide. The tidal elevations (as the sum of two terms: *Ocean Tide* and *Loading Tide*) were extracted from the Danmarks Tekniske Universitet ftp server: (ftp://ftp.space.dtu.dk/pub/DTU10/). *DTU10* was interpolated to the along-track positions of the track segment analysed.

3.2.2 Local hydrodynamic model: UCA2.5D

The two-dimensional (depth-averaged), two-layer, finite-difference, hydrodynamic model *UCA2.5D* (Izquierdo et al., 2001; Brandt et al., 2004) was developed specifically to reproduce the two-layer dynamics in the highly density-stratified environment of the Strait of Gibraltar. The model outputs are the depth-averaged horizontal currents in the upper and lower layers, as well as their respective top-limit heights (i.e., free-surface and interface depth). The curvilinear model grid extends from the easternmost area of the Gulf of Cadiz to the western half of the Alboran Sea, with a variable horizontal spatial resolution ranging from ~1 km in the eastern and western boundaries of the domain to ~125 m within the Strait of Gibraltar. The model currently runs in pre-operational mode and is forced at the open boundaries by the main semidiurnal (M_2, S_2) and diurnal (K_1, O_1) tidal constituents, as well as by surface wind and Mean Sea Level Pressure (MSLP) fields (Izquierdo et al., 2016) provided by the meteorological model MM5 (www2.mmm.ucar.edu). *UCA2.5D* has been extensively applied and validated in the Strait of Gibraltar, showing in general a good agreement with the observed hydrodynamics, including the mean interface depth and its tidal oscillations (Sein et al., 1998; Izquierdo et al., 2001; Brandt et al., 2004; Izquierdo et al., 2016).

3.3 Mean Sea Surface models

A mean sea surface (MSS) profile is subtracted to the along-track corrected sea surface height in order to get the anomalies (SLA). We used two sources of along-track MSS: (i) Global Mean Sea Surface: *DTU15MSS*; and (ii) Along-track Local Mean Sea Surface: *AT_Local_MSS*.

3.3.1 Global Mean Sea Surface: DTU15MSS

This mean sea surface model is an updated version of the previous *DTU10MSS* (Andersen and Knudsen, 2009; Andersen, 2010). The new version includes, globally, 4 years of CryoSat-2 data from its three modes of operation: Low Rate Mode (LRM), Synthetic Aperture Radar (SAR) and SAR-Interferometric (SAR-In). Data were extracted from the Danmarks Tekniske Universitet ftp server:

ftp://ftp.space.dtu.dk/pub/DTU15/1_MIN/ at 1-minute resolution grid. *DTU15MSS* was interpolated to the along-track positions of the track segment analysed.

3.3.2 Along-track Local Mean Sea Surface: AT_Local_MSS

An along-track Mean Sea Surface (*AT_Local_MSS*) based on ALES data was computed by interpolating the along-track Sea Surface Height (SSH) onto nominal tracks following the procedure explained in Passaro et al. (2014). We used the descending orbit #0360 combining all the overpasses from both the ERS-2 and Envisat missions with the same set of corrections. This approach brings several beneficial effects:

- Using two missions allows the computation of the anomalies in the study area, where the variability is higher, with a local mean sea level measured at the same track locations over a longer time span than from the Envisat mission alone;
- Using the same algorithm (ALES) and the same corrections as noted by Andersen and Scharroo (2011), the use of a MSS computed using altimetry data that are retracked with different algorithms and could therefore suffer from biases w.r.t. ALES data even in the open ocean prevents biases or differences that might otherwise show up as dynamic topography.

3.4 Experimental data sets

3.4.1 Tide gauge and bottom pressure data

The validation of the constituents of the global tidal model (*DTU10*) and of the local hydrodynamic model (*UCA2.5D*) was made using information available in the literature (García-Lafuente, 1986; Candela et al., 1990). We used the amplitude and phase of the main tidal constituents obtained from 11 *in-situ* instruments (tide gauges and bottom pressure sensors): Tarifa, SN, DN, DS, SS, Pta. Gracia, Pta. Kankoush, Pta. Carnero, Pta. Cires, Algeciras, and Ceuta (Figure 1).

The cross-strait sea level variability in the study area was also analysed using the measurements from two pressure tide gauges deployed at Ceuta and Tarifa by Puertos del Estado (http://www.puertos.es) (Figure 1). The recorded 5-minute resolution time series of water column height from 2002 to 2010 were smoothed and decimated to standard hourly values (Godin, 1972), and the resulting hourly series were subjected to harmonic analysis (Foreman and Henry, 1989), in order to obtain the amplitude and phase harmonic constants for the resolvable tidal constituents, as well as the mean sea level relative to the instrument. The difference between the original time series and the corresponding tidal prediction computed from the obtained tidal harmonics, usually known as 'residual height', is assumed to be free of any tidal contribution, and the resulting residual series from the two locations were used to obtain the sea level differences between them, in order to analyse their relationship with the wind conditions.

3.4.2 Bathymetry

Bathymetry has a high spatial resolution of 50 m, provided by the Spanish Navy Hydrographic Institute. It is available by request to the EMODNET Project web page: http://www.emodnet-bathymetry.eu.

3.4.3 Wind velocity

The zonal component of the wind velocity (u) used in the study was extracted from the hourly time series of 10-m height wind speed and direction from October 2002 to October 2010, recorded by the weather station deployed by the Spanish Meteorological Agency (AEMET) at Tarifa (Figure 1).

3.5 Absolute Dynamic Topography (*ADT*)

The sea level above geoid is commonly known as Absolute Dynamic Topography and can be obtained from the sum of two terms: along-track Sea Level Anomaly (*AT_SLA*) and along-track Mean Dynamic Topography (*AT_MDT*):

$$AT\_ADT = AT\_SLA + AT\_MDT \quad (2)$$

AT_SLA was obtained using the corrections presented in subsection 3.1 (Eq. 1). *AT_MDT* was obtained from two sources of Mean Dynamic Topography: *Global / Local MDT*.

3.5.1 Global MDT

We used the most updated version available of the DTU Mean Dynamic Topography. *DTU15MDT* (Knudsen et al., 2016) were extracted from the ftp server: ftp://ftp.space.dtu.dk/pub/DTU15/1_MIN/ at 1-minute resolution grid. In this model the newer version of the gravity field (EIGEN-6C4) has been combined with *DTU15MSS* to obtain the global Mean Dynamic Topography.

3.5.2 Local MDT

The local MDT was obtained as the time mean of 1-year long sea surface height hourly output from the local hydrodynamic model: *UCA2.5D* (Izquierdo et al., 2001). Brandt et al. (2004) validated this numerical model in the study area in terms of current velocity (current-meter moorings and the inverse tidal model of Baschek et al. 2001), and sea surface elevation (bottom pressure tide gauges). In general, the authors found a good level of agreement between the numerical model, the observations and the inverse tidal model of Baschek et al. (2001).

4. Results

4.1 Assessment of the models used for altimeter corrections

4.1.1 DTU10 vs. local hydrodynamic model

The performance of the global / local models in the Strait is analysed in detail. The global tidal model *DTU10* was already assessed in a previous work (Gómez-Enri et al., 2016). The authors compared the main constituents derived from a tide gauge located at Tarifa harbour with the constituents provided by *DTU10* (at the tide gauge location) estimating a root square sum (*RSS*) of 4.6 cm, following Oreiro et al. (2014). We extended this analysis by assessing the constituents of the models (*DTU10* and *UCA2.5D*) estimating the *RMS* of the differences and the *RSS* of the main constituents: M_2 and S_2 (semidiurnals), K_1 and O_1 (diurnals) using information from a few tide gauges and bottom pressure instruments located within the Strait of Gibraltar (Figure 1). The results are summarized in Table 1. Overall, both models show similar results, in terms of *Total_RSS* (4.3 / 4.2 cm for *DTU10* / *UCA2.5D*, respectively); we observe the lowest *RSS* (below 2.0 cm) in a few stations: DN and Algeciras (*DTU10*), SS and Ceuta (*UCA2.5D*). In the case of *DTU10* this might be due to the fact that these stations are likely assimilated in the model. The comparison with the closest stations to the satellite track (Pta. Carnero and Pta. Cires) gives similar *RSS* in Pta. Cires for both models and slightly better results for *DTU10* in Pta. Carnero.

The analysis of the models in the study area indicates that *DTU10* (globally and freely available) shows a similar level of accuracy as the local hydrodynamic model. For this reason, we used the global model to de-tide the sea level signals to estimate the *AT_SLA*.

4.1.2 Spatial variability of AT_SLA

Not all the overpasses of the satellite yield usable data – some cycles are missing due to acquisition problems or other platform issues and in a few cases the data were collected with a lower radar pulse bandwidth (20 MHz or 80 MHz instead of the usual 320 MHz over ocean), which makes them not accurate enough for oceanographic investigation. The number of overpasses with valid 320-MHz data is 78. The removal of outliers was made in two steps: (i) Only the *SLA* values between [-2.5 2.5] (m) were retained; and (ii) All the absolute *SLA* values greater than 3 times the standard deviation of the mean along-track profile were considered as outliers. Finally, a five-elements running mean was applied to the valid *AT_SLA* to remove high frequency noise (equivalent to 1.75 km).

Table. 1. *RMS* of the differences of the main constituents from the global model DTU10 and local hydrodynamic model UCA2.5D with some tide gauge and bottom pressure instruments in the study area. The *RSS* and *Total_RSS* are also shown.

	***RMS* differences (cm)**				***RSS* (cm)**
	M_2	**S_2**	**K_1**	**O_1**	
Station/Tide Gauge	**DTU10 / UCA2.5D**				**DTU10 / UCA2.5D**
Tarifa	4.9 / 5.6	1.9 / 2.0	0.6 / 1.2	1.3 / 1.7	5.5 / 6.3
SN	4.9 / 5.6	2.1 / 1.9	0.4 / 1.0	0.6 / 1.1	5.4 / 6.1
DN	0.8 / 4.8	1.0 / 2.4	0.3 / 0.9	1.0 / 0.7	1.7 / 5.5
DS	4.0 / 2.4	0.2 / 0.9	0.9 / 1.0	0.9 / 1.2	4.2 / 3.0
SS	5.5 / 1.3	2.0 / 0.3	1.7 / 1.0	1.6 / 0.8	6.3 / 1.9
Pta. Gracia	3.6 / 6.3	2.2 / 2.2	1.1 / 1.5	0.7 / 1.5	4.4 / 7.0
Pta. Kankoush	7.0 / 3.4	1.5 / 1.3	0.8 / 1.7	1.2 / 1.8	7.3 / 4.5
Pta. Carnero	1.0 / 2.4	0.9 / 0.03	0.5 / 0.5	1.3 / 0.7	2.0 / 2.6
Pta. Cires	4.6 / 4.6	1.2 / 1.3	0.5 / 0.8	1.1 / 0.6	4.9 / 4.9
Algeciras	0.6 / 2.8	0.4 / 0.2	0.7 / 0.3	0.6 / 0.7	1.2 / 2.9
Ceuta	3.6 / 0.8	1.8 / 0.4	0.1 / 0.4	0.2 / 0.3	4.0 / 1.0
					Total_RSS 4.3 / 4.2

As shown from the results in Table 1 the accuracy of the global tidal model *DTU10* needs to be assessed with care in the Strait of Gibraltar. This model does not include tidal constituents of longer periods than semidiurnal and diurnals (Cheng and Andersen, 2011). Two of the most important constituents of longer periods in the Strait are: M_{sf} (lunisolar synodic fortnightly) and M_m (lunar monthly). The harmonic analysis made to de-tide the in-situ time series at Ceuta and Tarifa stations (Figure 1), included these and others constituents. We analysed their magnitude in the vicinity of the satellite track segment. To do this, we obtained their amplitude and phase from the literature (Garcia-Lafuente et al., 1990) at the closest in-situ stations to the satellite pass: Pta. Carnero and Pta. Cires (Figure 1). The values are summarised in Table 2. The fortnightly constituent (M_{sf}) has a small and similar amplitude at both sides of the Strait showing a similar phase. The amplitude of the lunar monthly (M_m) is of the same order of magnitude at both stations, but they are in phase opposition. This comparison might indicate a small impact of not using longer period constituents to de-tide the sea level with the global model DTU10 in the Strait.

Table 2. Amplitude and phase of M_{sf} and M_m constituents for Pta. Carnero and Pta. Cires tide gauge stations

	Pta. Carnero		**Pta. Cires**	
	Amplitude (cm)	*Phase (º)*	*Amplitude (cm)*	*Phase (º)*
$\mathbf{M_{sf}}$	2.5	92	1.4	40
$\mathbf{M_m}$	1.1	153	1.9	302

A visual inspection of the radargrams of the waveforms gave two main patterns in the leading edge area of the returned echoes: (i) 'stable' leading edge around the nominal tracking point; this was found in 30 out of 78 cycles; (ii) 'non-stable' undulated leading edge in the northern sector of the track segment; this was observed in 42 cycles. In 3 cycles we noted a strange behaviour in the leading edge and thermal noise areas. Finally, 3 cycles showed a short track segment. Thus, only 40% of cycles (30) were considered valid for further analysis. The radargrams of the waveform power of a rejected cycle (no. 6) and a valid cycle (no. 14) is presented in Fig. 2a and Fig. 2b, respectively. The undulated radargram is due to the known problems of the on-board tracker in keeping the signal within the analysis window in proximity of land (Gommenginger et al. 2011).

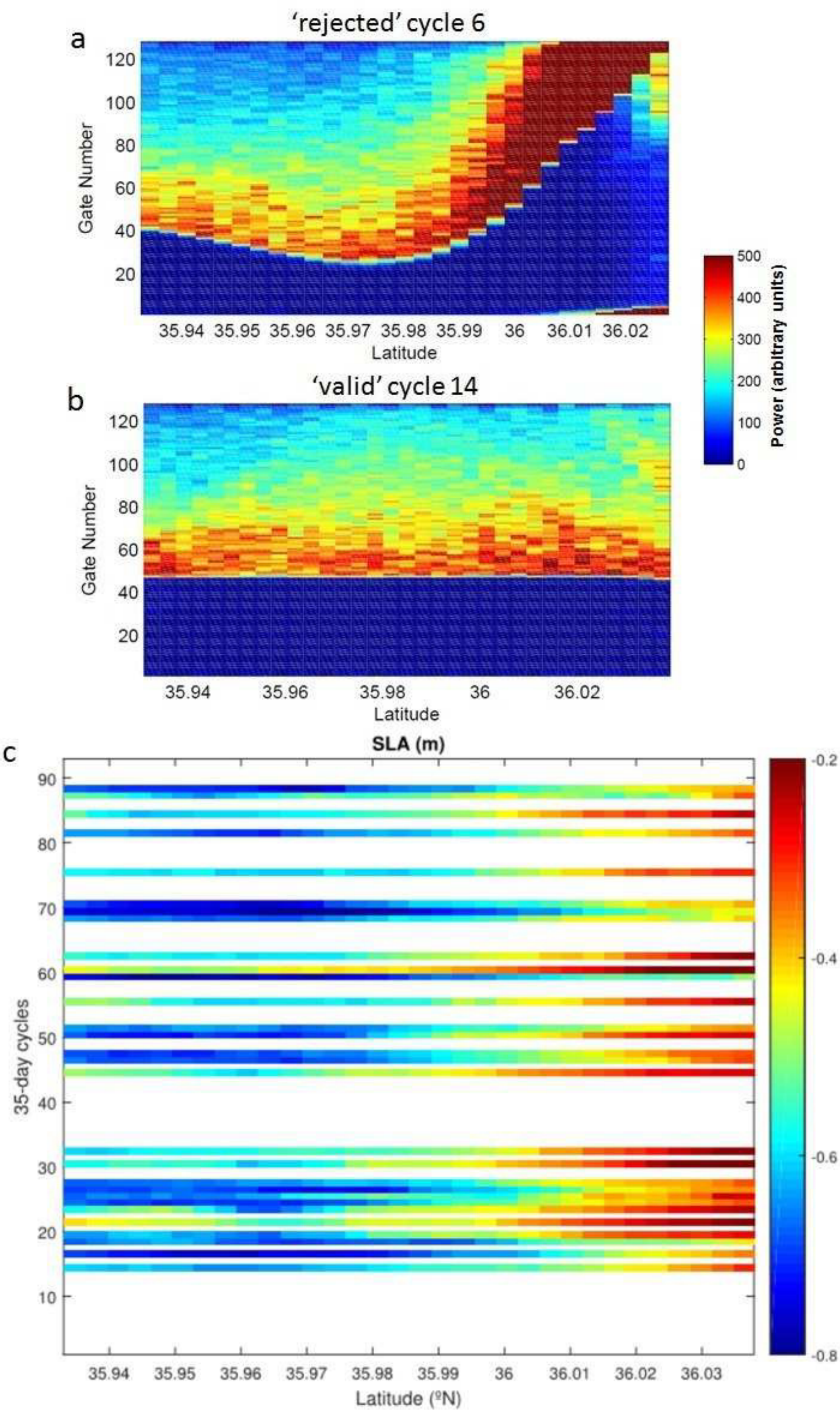

Figure 2. Radargram of the RA-2 radar waveform power for a rejected (Fig. 2.a) and a valid (Fig. 2.b) cycle. The cycle-by-cycle *AT_SLA* for valid cycles is shown in Fig. 2.c.

The cycle-by-cycle *AT_SLA* profiles after the data screening and the removal of invalid cycles due to unstable leading edges in the waveforms are shown in Fig. 2c. The sea level oscillates in the range: [-0.8 -0.2] m with a marked difference between the

African (lower sea level) and the Spanish (higher sea level) coasts. This behaviour is not in agreement with previous works made in the study area. Ross et al. (2000) indicated higher sea level on the southern side of the Strait. They used data from two tide gauges located in Ceuta (African coast) and Algeciras (Spanish coast) (Figure 1). The magnitude of this difference seems to range between 20 cm and 10 cm between maximal and submaximal exchange (Bormans and Garrett, 1989). A similar result was also reported by Stanichny et al. (2005).

One of the reasons that could explain this disagreement might be in the use of a global mean sea level (*DTU15MSS*) to estimate *AT_SLA*. The model, as the other global MSS models in the literature, is derived by merging several years of data from repeated tracks with nonrepeating data from geodetic missions using sophisticated interpolation techniques. The accuracy of these models is known to be degraded close to the coast (Andersen et al., 1999; Vignudelli et al., 2006), since the quality and the amount of the altimeter data used in the models is notably lower in the last ~25 km from the coast (Passaro et al. 2014; 2015), which means that the MSS values in the coastal zone are generally extrapolated (Andersen et al., 1999). This might be particularly relevant in our study area due to the lack of accurate along track high-resolution altimeter data in the past (Gómez-Enri et al., 2016). We investigated this by comparing the *AT_SLA* profiles obtained using the global (*DTU15MSS*) and the local (*AT_MSS*) mean sea levels. Figure 3 shows the average of *AT_SLA* over all valid cycles. Fig. 3a (*DTU15MSS*) gives a lower sea level in the African coasts (5-elements running mean applied). The ERS2 / Envisat derived mean sea surface gives an *AT_SLA* (Fig. 3b) with a marked positive cross-strait sea level difference between the African and Spanish coasts, which is in agreement with previous studies (Bormans and Garrett, 1989; Ross et al., 2000;

Stanichny et al., 2005). Thus, the 'local' mean sea level (*AT_MSS*) was selected in order to estimate the along-track Absolute Dynamic Topography (*AT_ADT*).

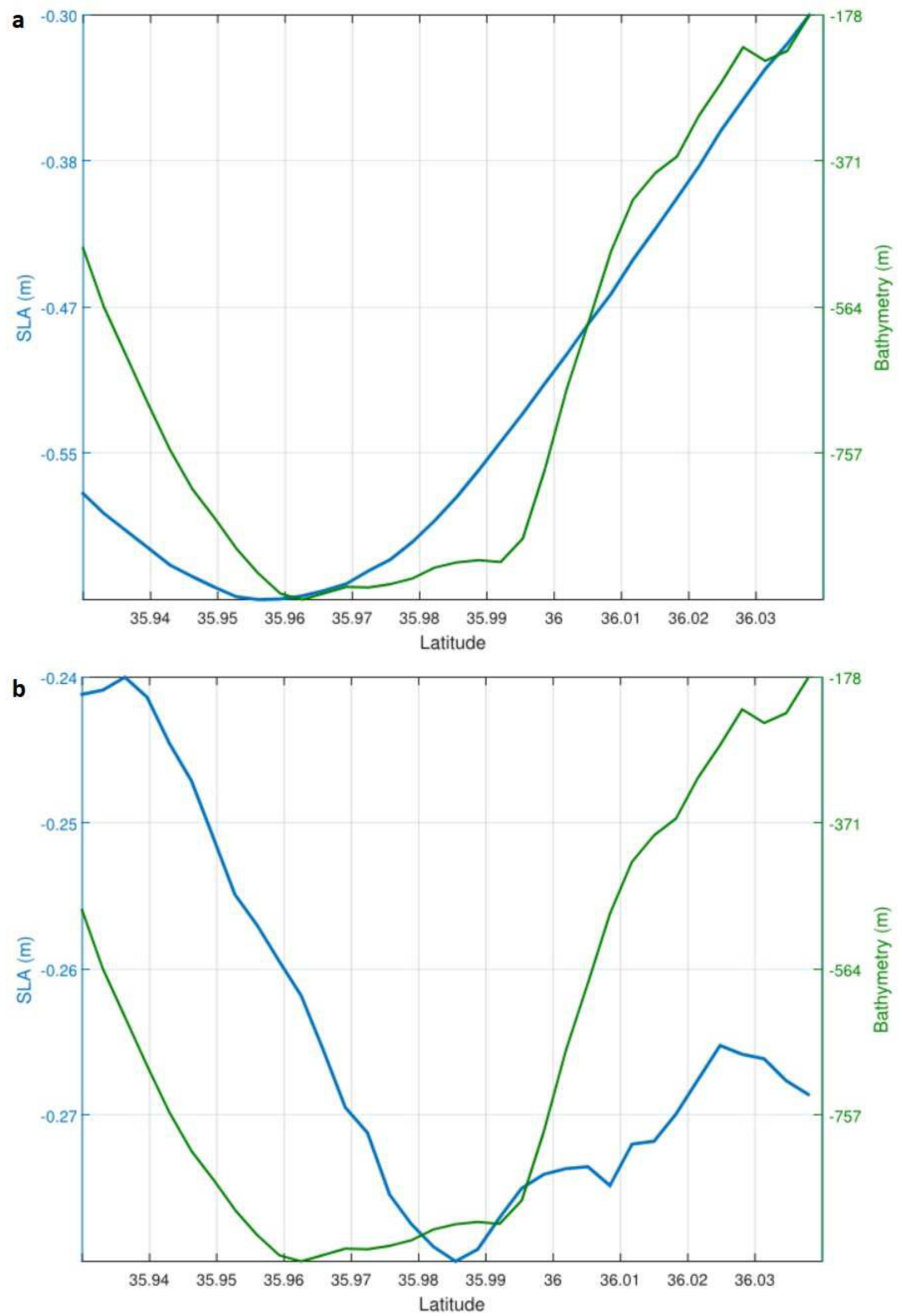

Figure 3. *AT_SLA* (5-elements running mean applied) for valid cycles using the global *DT15MSS* (Fig. 3.a) and the local *AT_MSS* (Fig. 3.b). The green line gives the bathymetry profile.

4.2 Cross-strait variability in the Strait of Gibraltar

4.2.1 Along-track ADT

As mentioned, we used two sources of *MDT* to compute the *AT_ADT* (Eq. 1). Figure 4 shows the *MDT_DTU15* (Fig. 4a) and *MDT_Local* (Fig. 4b) obtained from the local numerical model *UCA2.5D*. The magnitude of *MDT_DTU15* ranges between 4.5 - 7.5 cm, smaller than *MDT_Local*: -5 – 5 cm. The zonal variation of *MDT* (sea level decrease toward east) along the strait can be observed in both models but the local *MDT* shows a remarkable meridional cross-strait gradient. We also observe a difference in the magnitude of the mean along-strait sea level difference between the two entrances of the Strait. Thus, this difference is smaller than 2 cm for the global *MDT* but up to 6 cm for the local model. Also, the strong change in sea level pattern around Camarinal Sill shown in *MDT_Local* is not observed in *MDT_DTU15*. A possible explanation might lie in the fact that this global model does not resolve properly the baroclinic coupling between upper and lower layer flows (Brandt et al., 2004).

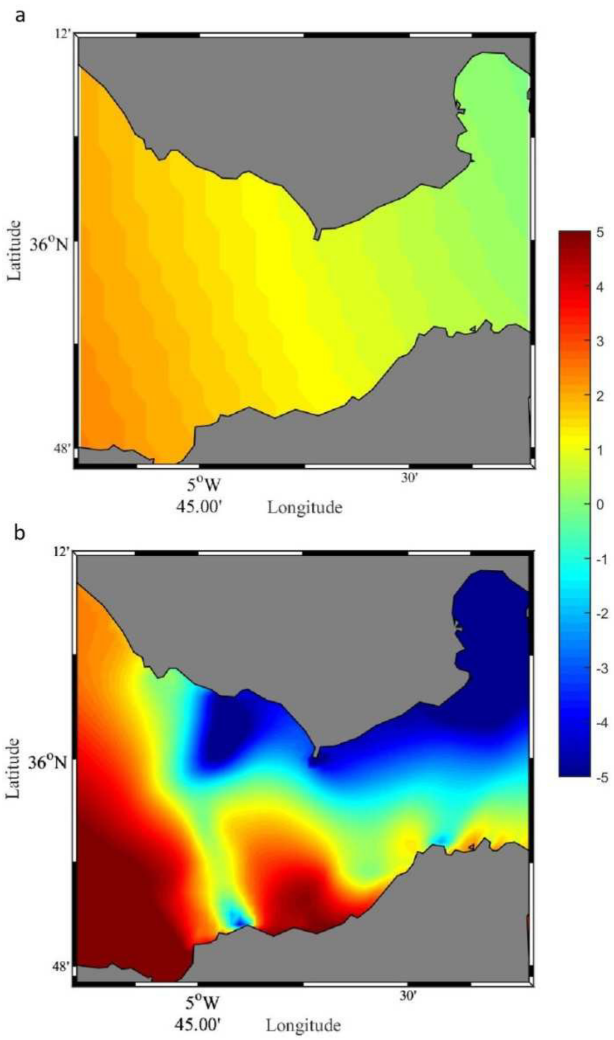

Figure 4. Mean Dynamic Topography (in cm) in the Strait of Gibraltar from the global model *MDT_DTU15* (5.a) and the local model *MDT_UCA2D* (5.b).

We recalculated along-track *ADT* (*AT_ADT*) following Eq. (2) using the *Local_MDT* (only for cycles with a 'stable' leading edge around the nominal tracking point). It can be seen a clear cross-strait sea level difference with higher sea level on the African side in most of the cycles (Fig. 5.a). Fig. 5.b gives the *AT_ADT* for a cycle (no. 51) with a positive cross-strait sea level difference. Also, inversions of the sea level differences between south and north sides are observed in some cycles. Fig. 5.c shows *AT_ADT* for cycle 50. We investigated this further by analysing its relationship with the wind regime.

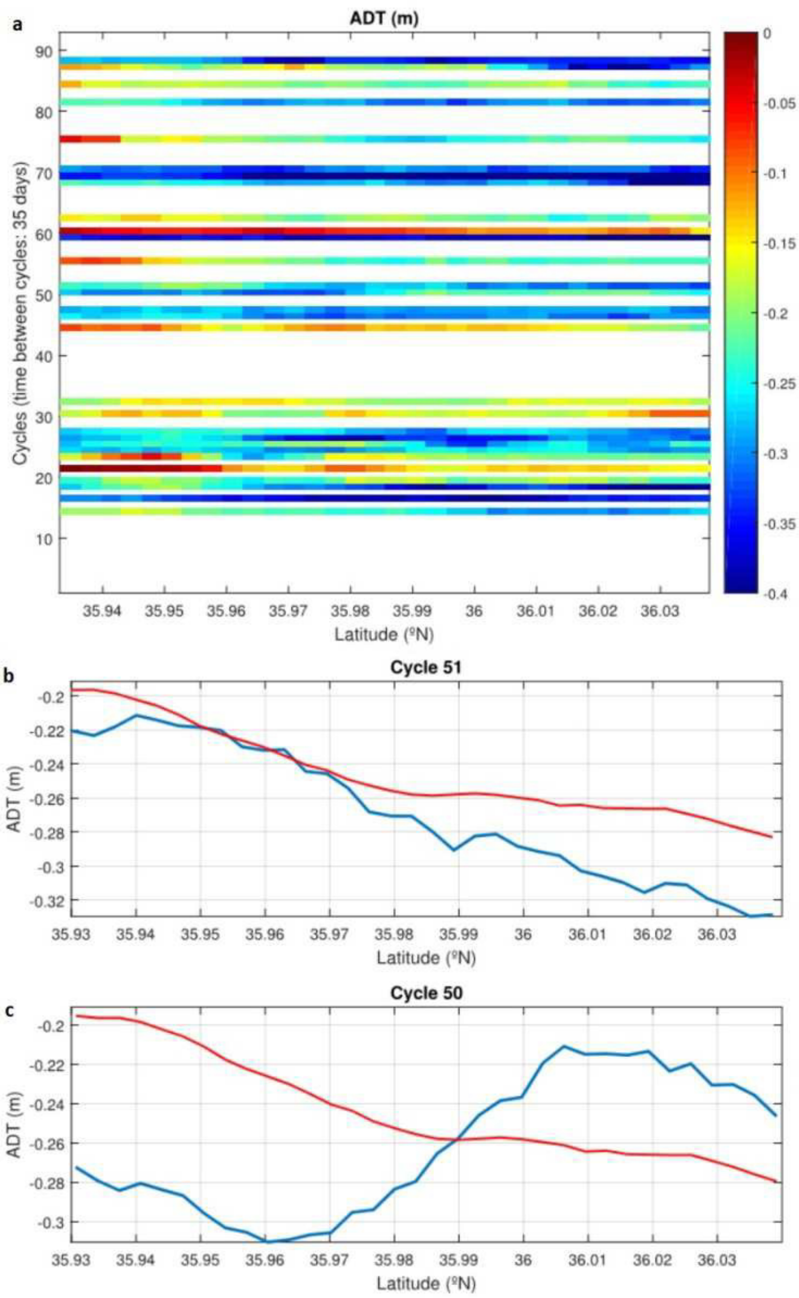

Figure 5. Cycle-by-cycle *AT_ADT* for valid cycles (Fig. 5.a). *AT_ADT* for cycle 51 (Fig. 5.b) and 50 (Fig. 5.c). The average of *AT_ADT* over all valid cycles is also shown in Fig. 5.b and 6.c (red line).

4.2.2 Inversion of the cross-strait sea level difference due to wind regime

We analysed the variability of the cross-strait sea level in the Strait of Gibraltar and its dependence on the wind regime. We first determine the response time of sea level to wind forcing following an empirical approach: the wind mean zonal component

($\hat{u}$) was calculated as the average u value from a time interval (N_h) starting immediately before the pass of the satellite (about 10:46 UTC time). N_h was ranging from 1 to 48 hours before that time. The time response selected was that corresponding to the averaging interval giving the maximum correlation coefficient between the calculated zonal component ($\hat{u}$) and the sea level difference between the two tide gauge stations. Figure 6 gives the correlation coefficients (p_value < 0.05) between $\hat{u}$ and the sea level gradient for increasing N_h. The best correlation (r = 0.812) was found for N_h = 2. Easterly/westerly winds (the so-called Levante/Poniente winds, respectively) give negative/positive $\hat{u}$ component.

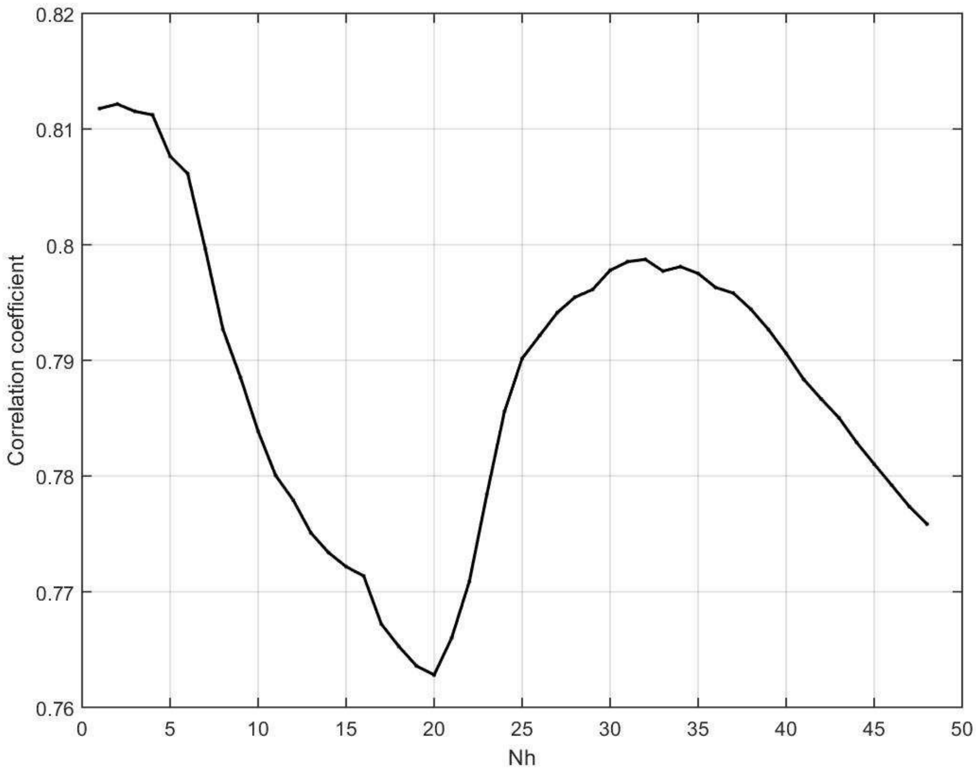

Figure 6. Correlation coefficient between the calculated zonal component ($\hat{u}$) and the sea level gradient between the two tide gauge stations (Ceuta and Tarifa) for increasing time intervals (N_h).

We obtained the sea level difference between the south and north sides of the Strait from altimetry and the two tide gauges located in Ceuta and Tarifa (Figure 1). The sea level difference from altimetry was obtained by estimating the cross-strait sea level slope using the starting and ending points of the linear fit made to the *AT_ADT* profiles. We found 8 out of 30 cycles with a small confidence level and were rejected in the analysis. The relationship between $\hat{u}$ and the sea level differences are shown in Figure 7 for altimeter (Fig. 7.a) and tide gauge data (Fig. 7.b). Negative differences indicate the inversion of the sea level difference between the southern and northern sectors of the Strait. This is clearly seen during easterlies in the two datasets, more evident in the tide gauge data, where the correlation coefficient is remarkably high (0.82). The inversion is due to the Ekman transport during strong easterlies. As mentioned, this is in agreement with previous observations in the study area. Stanichny et al. (2005) analysed correlation between the sea level gradient among tide gauges located in Ceuta, Algeciras and Tarifa and the zonal wind component of velocity. The authors found negative cross-strait differences during severe easterlies and a notably similar correlation coefficient (0.85). This effect of along-strait winds in the sea level difference across the Strait is further supported by the results of a process-study simulation carried out with UCA2.5D (Reyes, 2015). As compared to the no wind control solution, a constant easterly wind of 10 $m \cdot s^{-1}$ originates a sea level rise between 2 and 5 cm from Tarifa to Gibraltar, with a cross-strait sea-level difference of less than 7 cm at the eastern entrance of the Strait. In the case of a constant westerly wind of equal magnitude, this cross-strait sea-level difference is 12 cm.

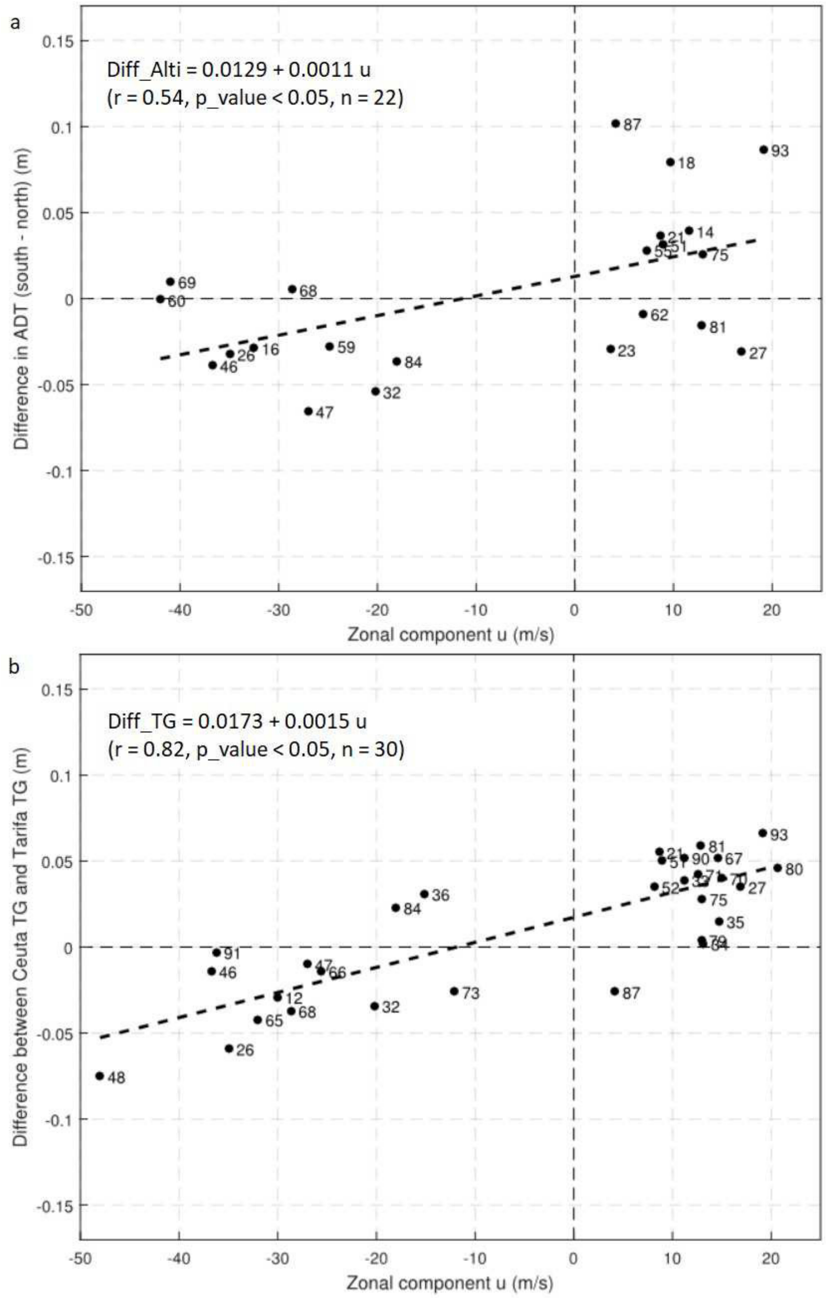

Figure 7. Cross-strait sea level differences between the African and Spanish coasts as a function of the mean zonal *û* component of the wind. Fig. 7.a gives the comparison using altimeter data and Fig. 7.b in-situ data. The numbers indicate the cycle number of the satellite pass.

5. Discussion

Our work was focused on the use of an accurate coastal sea level product from a pulse-limited altimeter (RA-2) in the Strait of Gibraltar. We have highlighted how the studies that look at spatial SLA profiles should take particular care of the MSS adopted.

We have shown (Figure 3) that even the use of a dedicated retracking procedure might not be able to provide a realistic sea level profile if the MSS used to extract the anomaly is based on standard products. There are at least two explanations for this. Firstly, the standard products are severely flagged in the coastal zone to avoid the risk of erroneous retrievals, which means that a global MSS model is probably characterised by strong data interpolation in the absence of local sea level data in areas such as the Strait of Gibraltar. Secondly, the use of different geophysical corrections in the computation of the global MSS w.r.t. the corrections used in the reprocessed SSH might leave unrealistic features when deriving the anomalies. This is for example the case of corrections with different spatial resolutions: for example, the Wet Tropospheric Correction from the radiometer rather than from an atmospheric model, or the Dynamic Atmosphere Correction forced with the operational ECMWF atmospheric model rather than with the ERA-Interim Reanalysis. These problems have been mentioned by Andersen and Scharroo (2011), and more recently by Han et al. (2017), but the Coastal Altimetry community has up to now overlooked the problem, which becomes of urgent matter nowadays, when the discipline is mature for oceanographic exploitation.

A possible future extension of this work would be the use of SAR mode altimetry from CryoSat-2 and Sentinel-3. The accuracy of current delay-Doppler missions: CryoSat-2 SIRAL and Sentinel-3A SRAL (already joined by Sentinel-3B) in terms of sea level has not been quantified in the study area. A thorough validation exercise of CryoSat-2 SIRAL data was performed by Gómez-Enri et al. (2017) in the eastern shelf of the Gulf of Cadiz (western end of the Strait). They concluded that the quality of CryoSat-2 20-Hz SLA data was comparable to conventional altimetry (Saral AltiKa 20-Hz data) in the coastal strip of the Gulf. However, the complexity of the

Strait of Gibraltar precludes the use of SAR altimetry missions for scientific exploitation before performing their validation with in-situ tide gauge data. The unique orbital configuration of the CryoSat-2 mission (369-days repeated cycle with a 30-days sub-orbital cycle) would allow a geographically distributed assessment of the cross-strait variability of the sea level in the Strait and its relationship with the wind regime. In addition to this, the 27-days orbital cycle of Sentinel-3A gives two tracks (one ascending and one descending) very close to the Envisat track analysed in this work with the cross-over at Algeciras city, north of Punta Carnero (Figure 1). This convenient sampling by Sentinel-3A combined with its SAR mode should allow a better knowledge of the hydrodynamic processes in the eastern side of the Strait of Gibraltar. For both CryoSat-2 and Sentinel-3, the use of a local mean sea surface to obtain the anomalies is needed.

6. Conclusions

The cross-strait variability in the eastern side of the Strait of Gibraltar and its relation to the wind regime has been analysed. We estimated the sea level differences between the southern and northern sector of the Strait and analysed their variability as a function of the zonal component of the wind. To do this, we estimated the absolute dynamic topography from the sea level anomalies obtained using along-track SLA (Envisat RA-2 descending track #0360) based on ALES reprocessing and improved geophysical corrections. The sea level differences and its dependence with the wind regime were compared with the outputs of two tide gauges located at both sides of the Strait. The main conclusions are summarised as follows.

The global mean sea level *DTU15MSS* does not take into account some of the particularities of such a complicated zone as the Strait of Gibraltar. Our results show that its use to compute the sea level anomalies might hide some of the sea level variability, and hence complicate their oceanographic interpretation. We have demonstrated that a local mean sea level (*AT_Local_MSS*) based on ALES reprocessing of ERS2/Envisat descending track #0360 along-track sea surface heights, gives a more realistic cross-strait variability in the Strait improving the analysis of the hydrodynamic processes in the area. The global tidal model *DTU10* shows a good performance in the Strait of Gibraltar to de-tide altimetric records. The mean *RSS* of the main constituents obtained with *DTU10* and 11 stations is 4.3 cm very similar to the *RSS* using a local hydrodynamic model (*UCA2.5D*) (4.2 cm).

The cross-strait variability obtained between the southern (Pta. Cires) and northern (Pta. Carnero) eastern zone of the Strait of Gibraltar is highly dependent on the wind regime. The analysis of the along-track absolute dynamic topography showed a positive correlation with the zonal component of the wind. The difference between the sea level in the southern and northern segments of the altimeter track gives positive / negative differences under westerlies / easterlies conditions. The inversion (negative) of that difference is related to severe easterlies as a result of the Ekman transport. This contributes to the modulation of the water exchange through the Strait of Gibraltar, weakening the Atlantic water inflow toward the Mediterranean Sea.

Coastal altimeter data are ready for exploitation in the coastal zone. Data accuracy needs to be continuously assessed near the shore, especially the products obtained from present altimeter (conventional and delay-Doppler) missions. The Strait of Gibraltar, the unique connection between the Mediterranean Sea and the Atlantic Ocean, plays an important role in their water exchange and its complexity has been thoroughly investigated for many years using ground-truth instruments and its hydrodynamic processes have been modelled. We have demonstrated here that satellite altimetry gives accurate sea level measurements in the Strait, and hence helps to a better knowledge of its hydrodynamic processes. We have also shown that, at least regionally, coastal altimetry can be used to significantly improve the knowledge of the MSS in the coastal zone. There is therefore a strong need to perform an impact assessment looking at the differences between current global MSS models and along-track MSS computed using reprocessed dataset such as ALES in other regions. High quality satellite-based altimeter with finer along-track spatial resolutions from SAR-mode missions such as Sentinel-3A/B should be incorporated to the experimental datasets available in the area.

ACKNOWLEDGMENTS

The authors are thankful to the Spanish Instituto Hidrográfico de la Marina (IHM) for the bathymetric dataset, and the Spanish Puertos del Estado for the tide gauge data at Tarifa and Ceuta. Special thanks to Ole B. Baltazar (Denmark Technological University) for his comments on the global tidal model DTU10. This work was partially funded by the OCASO-Interreg POCTEP project.

REFERENCES

Andersen, O. B. (1999). The DTU10 Gravity field and Mean sea surface. Presented at the Second International Symposium of the Gravity Field of the Earth (IGFS2). Fairbanks, Alaska.

Andersen, O. B. & Knudsen, P. (2009). The DNSC08 mean sea surface and mean dynamic topography. *Journal of Geophysical Research-Oceans*. doi: 10.1029/2008JC005179.

Andersen, O. B., Stenseng, L., Piccioni, G. & Knudsen, P. (2016). The DTU15 MSS (Mean Sea Surface) and DTU15LAT (Lowest Astronomical Tide) reference surface. *Presented at the ESA Living Planet Symposium.* Prague, Czech Republic.

Andersen, O. B. & Scharroo, R. (2011). Range and geophysical corrections in coastal regions: and implications for mean sea surface determination. In S. Vignudelli, A. Kostianoy, P. Cipollini & J. Benveniste (Eds.), *Coastal Altimetry* (pp. 103-145). Springer, Berlin, Heidelberg. doi: 10.1007/978-3-642-12796-0_5

Bascheck, B., Send, U., García-Lafuente, J., & Candela, J., (2001). Transport estimates in the Strait of Gibraltar with a tidal inverse model. *Journal of Geophysical Research*, 106 (C12), 31033-31044. doi: 10.1029/2000JC000458.

Bormans, M., & Garrett, C., (1989). The effects of nonrectangular cross section, friction, and barotropic fluctuations on the exchange through the Strait of Gibraltar. *Journal of Physical Oceanography*, 19 (10), 1543-1557. doi: 10.1175/1520-0485(1989)019<1543:TEONCS>2.0.CO;2.

Brandt, P., Rubino, A., Sein, D. V., Baschek, B., Izquierdo, A., & Backhaus, J. O., (2004). Sea level variation in the Western Mediterranean studied by a numerical tidal model of the Strait of Gibraltar. *Journal of Physical Oceanography*. doi: 10.1175/1520-0485(2004)034<0433:SLVITW>2.0.CO;2.

Brockley, D. J., Baker, S., Féménias, P., Martínez, B., Massmann, F. H., Otten, M., Paul, F., Picard, B., Prandi, P., Roca, M. & Rudenko, S. (2017). REAPER: Reprocessing 12 Years of ERS-1 and ERS-2 Altimeters and Microwave Radiometer Data. *IEEE Transactions on Geoscience and Remote Sensing*, 55 (5506-5514). doi: 10.1109/TGRS.2017.2709343.

Brown, S., (2010). A Novel Near-Land Radiometer Wet Path-Delay Retrieval Algorithm: Application to the Jason-2/OSTM Advanced Microwave Radiometer. IEEE Transactions on Geoscience and Remote Sensing, 48 (4), 1986-1992. doi: 10.1109/TGRS.2009.2037220

Calafat, F. M., Chambers, D. P., & Tsimplis, M. N. (2012). Mechanisms of decadal sea level variability in the eastern North Atlantic and the Mediterranean Sea, *Journal of Geophysical Research*, 117(C9), C09022. doi: 10.1029/2012JC008285.

Candela, J., Winant, C. D., & Bryden, H. L. (1989). Meteorologically forced subinertial flows through the Strait of Gibraltar. *Journal of Geophysical Research*, 94, 12667–12674. doi: 10.1029/JC094iC09p12667.

Candela, J., (1990). The barotropic tide in the Strait of Gibraltar. In L. J. Pratt (Ed.), *The Physical Oceanography of Sea Straits* (pp. 457-475), The Netherlands: Kluwer Academic Publishers. doi: 10.1007/978-94-009-0677-8_22.

Candela, J. (2001). Mediterranean water and ocean circulation. In G. Siedler et al. (Eds.), *Ocean Circulation and Climate: Observing and Modelling the Global Ocean* (pp. 419-429), Academic Press

Carrère, L. & Lyard, F. (2003). Modeling the barotropic response of the global ocean to atmospheric wind and pressure forcing - comparisons with observations. *Geophysical Research Letters*, 30, 1275. doi: 10.1029/2002GL016473.

Cheng, Y., & Andersen, O. B. (2011). Multimission empirical ocean tide modelling for shallow waters and polar seas, *Journal of Geophysical Research-Oceans*. doi: 10.1029/2011JC007172.

Cipollini, P., Benveniste, J., Birol, F., Fernandes, M. J., Obligis, E., Passaro, M., Strub, P. T., Valladeau, G., Vignudelli, S., & Wilkin, J. (2017). Satellite Altimetry in coastal regions. In D. Stammer & A. Cazenave (Eds), *Satellite altimetry over oceans and land surfaces* (pp. 343-380), (Earth observation of global changes book series), CRC Press Taylor & Francis, London, UK.

Cipollini, P., Calafat, F. M., Jevrejeva, S., Melet, A., & Prandi, P. (2017). Monitoring the sea level in the coastal zone with satellite altimetry and tide gauges, *Surveys in Geophysics*, 38, 33–57. doi: 10.1007/s10712-016-9392-0.

Copernicus Marine Environment Monitoring Service (CMEMS). (2017). Product User Manual, Ref.: CMEMS-SL-PUM-008-032-051, EU Copernicus Marine Service, 46 pp.

Dong, C., Xu, G., Han, G., Chen, N., He, Y., & Chen, D. (2018). Identification of tidal mixing fronts from high-resolution along-track altimetry data. *Remote Sensing of Environment*, 209, 489-496. doi: 10.1016/j.rse.2018.02.047.

ESA. (2007). ENVISAT RA2/MWR Product Handbook. Issue 2.2. https://earth.esa.int/pub/ESA_DOC/ENVISAT/RA2-MWR/ra2-mwr.ProductHandbook.2_2.pdf

Foreman, M. G. G., & Henry, R. F. (1989). The harmonic analysis of tidal model time series. *Advances in Water Resources*, 12 ()3, 109-120. doi: 10.1016/0309-1708(89)90017-1.

Fukumori, I., Menemenlis, D., & Lee, T. (2007). A near-uniform basin-wide sea level fluctuation of the Mediterranean Sea, *Journal of Physical Oceanography*, 37(2), 338-358. doi: 10.1175/JPO3016.1.

Garcia-Lafuente, J. (1986). Variabilidad del nivel del mar en el Estrecho de Gibraltar. Mareas y oscilaciones residuales. *Phd. Thesis*, Instituto Español de Oceanografía, Fuengirola, Málaga, Spain, 154 pp.

Garcia-Lafuente, J., Almazán, J. L., Castillejo, F., Khribeche, A., & Hakimi, A. (1990). Sea level in the Strait of Gibraltar: Tides. *International Hydrographic Review*, LXVII (1), 111-130.

Garcia-Lafuente, J., Delgado, J. & Criado F. (2002). Inflow interruption by meteorological forcing in the Strait of Gibraltar. *Geophysical Research Letters*, 29. doi: 10.1029/2002GL015446.

Garrett, C., Bormans, M., & Thompson, K. (1990). Is the exchange through the Strait of Gibraltar Maximal or Submaximal. In L. J. Pratt (Ed.). *The Physical Oceanography of Sea Straits*, Kluwer Academic Publishers, Dordrecht, The Netherlands.

Gill A. E., & Clarke A. J. (1974). Wind-induced upwelling, coastal currents and sea-level changes. *Deep-Sea Research*, 21, 325-345. doi: 10.1016/0011-7471(74)90038-2.

Godin, G. (1972). The analysis of tides. The University of Toronto Press, Toronto, Canada.

GCOS (2016). The Global Observing System for Climate: Implementation needs. World Meteorological Organization.

Gómez-Enri, J., Cipollini, P., Passaro, M., Vignudelli, S., Tejedor, B. & Coca, J. (2016). Coastal Altimetry Products in the Strait of Gibraltar, *IEEE Transactions on Geosciences and Remote Sensing*. doi: 10.1109/TGRS.2016.2565472.

Gómez-Enri, J., Vignudelli, S., Cipollini, P., Coca, J. & Gonzalez, C. J. (2017). Validation of CryoSat-2 SIRAL sea level data in the Eastern continental shelf of the Gulf of Cadiz. *Advances in Space Research*, *in press*, doi: 10.1016/j.asr.2017.10.042.

Gommenginger, C. P., Thibaut, P., Fenoglio-Marc, L., Quartly, G. D., Deng, X., Gómez-Enri, J., Challenor, P. & Gao, Y. (2011). Retracking altimeter waveforms near the coasts - a review of retracking methods and some applications to coastal waveforms. In S. Vignudelli, A. Kostianoy, P. Cipollini & J. Benveniste (Eds.), *Coastal Altimetry* (pp. 61-101). Springer, Berlin, Heidelberg. doi: 10.1007/978-3-642-12796-0_4.

Han, G., Ma, Z., Chen, C., Chen, N., Yang, J., & Chen, D. (2017). Hurricane Isaac storm surges off Florida observed by Jason-1 and Jason-2 satellite altimeters. Remote Sensing of Environment, 198, 244-253. doi:10.1016/j.rse.2017.06.005.

Han, G., Ma, Z., Chen, D., DeYoung, B. & Chen, N. (2012). Observing storm surges from space: Hurricane Igor off Newfoundland. Scientific Reports, 2, 1010. doi:10.1038/srep01010.

Handoko E. Y., Fernandes, M. J. & Lazaro, C. (2017). Assessment of altimeter range and geophysical corrections and mean sea surface models – Impacts on sea level variability around the Indonesian Seas. *Remote Sensing* *9*(2), 102. doi:10.3390/rs9020102.

Hughes, C. W., R. J. Bingham, V. Roussenov, J. Williams & P. L. Woodworth (2015). The effect of Mediterranean exchange flow on European time mean sea level, *Geophysycal Research Lett*eers, 42, 466–474. doi: 10.1002/2014GL062654.

Izquierdo, A., Tejedor, L., Sein, D. V., Backhaus, O., Brandt, P., Rubino, A. & Kagan, B. A. (2001). Control variability and internal bore evolution in the Strait of Gibraltar: a 2-D two-layer model study, *Estuarine Coastal and Shelf Science*. doi: 10.1006/ecss.2000.0706.

Izquierdo, A., Kagan, B. & Sein, D. & Mikolajewicz, U. (2016). Modelling in the Strait of Gibraltar: from operational oceanography to scale interactions. *Fundamentalnaya i prikladnaya gidrofizika*. 9. 15-24.

Knudsen, P, Andersen, O. B. & Maximenko, N. (2016). The updated geodetic mean dynamic topography model – DTU15MDT. *Presented at the ESA Living Planet Symposium, 2016.* Prague, Czech Republic.

Lacombe, H. & Richez, C. (1982). The regime in the Strait of Gibraltar. In Jacques C.J. Nihoul (Ed.). *Hydrodynamics of Semi-Enclosed Seas* (pp. 13-73). Proceedings of the 13th International Liege Colloquium on Ocean Hydrodynamics, Elsevier Oceanography Serie. doi: 10.1016/S0422-9894(08)71237-6.

Landerer, F. W., & Volkov, D. L. (2013). The anatomy of recent large sea level fluctuations in the Mediterranean Sea. *Geophysycal Research Letters*, 40. doi:10.1002/grl.50140.

Legeais, J. F., Ablain, M., Zawadzki, L., Zuo, H., Johannessen, J. A., Scharffenberg, M. G., Fenoglio-Marc, L., Fernandes, M. J., Andersen, O. B., Rudenko, S., Cipollini, P., Quartly, G. D., Passaro, M., Cazenave, A. & Benveniste, J. (2018). An improved and homogeneous altimeter sea level record from the ESA Climate Change Initiative. *Earth System Science Data*, 10, 281-301, doi: 10.5194/essd-10-281-2018.

Lyard, F., Lefèvre, F., Letellier, T. & Francis, O. (2006). Modelling the global ocean tides: modern insights from FES2004. *Ocean Dynamics*. doi: 10.1007/s10236-006-0086-x.

Menemenlis, D., Fukumori, I., & Lee, T. (2007), Atlantic to Mediterranean sea level difference driven by winds near Gibraltar Strait. *Journal of Physical Oceangraphy*, 37, 359-376. doi:10.1175/JPO3015.1.

Mercier, F., Rosmorduc, V., Carrere, L., & Thibaut, P. (2010). Coastal and Hydrology Altimetry product (PISTACH) Handbook. CLS-DOS-NT-10-246, Issue 1.0, CNES.

Oreiro, F., D'Onofrio, E., Grismeyer, W., Fiore, M. & Saraceno, M. (2014). Comparison of tide model outputs for the northern region of the Antarctic Peninsula using satellite altimeters and tide gauge data. *Polar Science*, doi: 10.1016/j.polar.2013.12.001.

Passaro, M., Cipollini, P., Vignudelli, S., Quartly, G. D. & Snaith, H. N. (2014). ALES: A multi-mission adaptive subwaveform retracker for coastal and open ocean altimetry. *Remote Sensing of Environment*. doi: 10.1016/j.rse.2014.02.008.

Passaro, M., Cipollini, P. & Benveniste, J. (2015). Annual sea level variability of the coastal ocean: The Baltic Sea-North Sea transition zone. *Journal of Geophysical Research: Oceans*, 120 (4), 3061-3078. doi: 10.1002/2014JC010510.

Passaro M., Dinardo S., Quartly G. D., Snaith H. M., Benveniste J., Cipollini P. & Lucas B. (2016). Cross-calibrating ALES Envisat and CryoSat-2 Delay–Doppler: a coastal altimetry study in the Indonesian Seas. *Advances in Space Research*, 58(3), 289-303. doi: 10.1016/j.asr.2016.04.011.

Peng F, & Deng X. (2018). A new retracking technique for Brown peaky altimetric waveforms. *Marine Geodesy*, 41(2), 99-125. doi: 10.1080/01490419.2017.1381656.

Quartly, G. D., Legeais, J. F., Ablain, M., Zawadzki, L., Fernandes, M. J., Rudenko, S., Carrère, L., García, P. N., Cipollini, P., Andersen, O. B., Poisson, J. C., Mbajon Njiche, S., Cazenave, A. & Benveniste, J. (2017). A new phase in the production of quality-controlled sea level data. *Earth System Science Data*, 9, 557-572. doi: 10.5194/essd-9-557-2017.

Reid J. L. (1979). On the contribution of the Mediterranean Sea outflow to the Norwegian-Greenland Sea. *Deep Sea Research Part A. Oceanographic Research Papers*, 26(11), 1199-1223. doi: 10.1016/0198-0149(79)90064-5.

Reyes, M. M. (2014). Modelado de alta resolución para el estudio de la respuesta oceánica al forzamiento del viento en el estrecho de Gibraltar. *Ph. D. Thesis*. University of Cadiz. Spain. *Available in: https://rodin.uca.es/xmlui/handle/10498/17501*.

Roscher R., Uebbing B. & Kusche J. (2017). STAR: Spatio-temporal altimeter waveform retracking using sparse representation and conditional random fields. *Remote Sensing of Environment,* 201, 148-64. doi:

Ross, T., Garrett, C. & Le Traon, P. Y. (2000). Western Mediterranean sea-level rise: Changing exchange flow through the Strait of Gibraltar. *Geophysical Research Letters*. doi: 10.1029/2000GL011653.

Sein, D., Backhaus, J. O., Brandt, P., Izquierdo, A., Kagan, B., Rubino, A. & Tejedor, L. (1998). Flow exchange and tidally induced dynamics in the Strait of Gibraltar derived from a two-layer, boundary-fitted coordinate model. *Presented at the Oceanic Fronts and Related Phenomena*. doi: 10.13140/RG.2.1.2572.1208.

Stanichny, S., Tigny, V., Stanichnaya, R., & Djenidi, S. (2005). Wind regime upwelling along the African coast of the Strait of Gibraltar. *Geophysical Research Letters*, 32 (4), doi: 10.1029/2004GL021760.

Tejedor, L., Izquierdo, A., Sein, D.V. & Kagan, B.A. (1998). Tides and tidal energetics of the Strait of Gibraltar: a modelling approach. *Technophysics* 298, 333 – 347. doi: 10.1016/S0040-1951(98)00110-3.

Vignudelli, S., Kostianoy, A., Cipollini, P. & Benveniste, J. B. (Eds.). (2011). *Coastal Altimetry*. Springer, Berlin, Heidelberg. doi: 10.1007/978-3-642-12796-0.

Vignudelli S., Snaith H. M., Lyard F., Cipollini P., Birol F., Bouffard J. & Roblou L. (2006). Satellite radar altimetry from open ocean to coasts: challenges and perspectives. *Presented at the Photo-Optical Instrumentation Engineers (SPIE) Asia-Pacific Remote Sensing Symposium*, Panaji, Goa, India. doi:10.1117/12.694024, 2006.

Volkov, D. L., & Landerer, F. W. (2015). Internal and external forcing of sea level variability in the Black Sea. *Climate Dynamics*, 45 (9-10), 2633-2646. doi:10.1007/s00382-015-2498-0.

Volkov, D. L., Johns, W. E., & Belonenko, T. V. (2016). Dynamic response of the Black Sea elevation to intraseasonal fluctuations of the Mediterranean sea level. *Geophysical Research Letters* 43, 283-290. doi: 10.1002/2015GL066876.

Xi-Yu, X., Birol, F. & Cazenave, A. (2018). Evaluation of coastal sea level offshore Hong Kong from Jason-2 altimetry. *Remote Sensing 10* (2), 282. doi: 10.3390/rs10020282.

List of Figure Captions

Figure 1. Study area: The Strait of Gibraltar between Europe and Africa. Colour scale indicates the bathymetry (in meters). Also shown the location of ERS-2 / Envisat descending track #0360 (the track segment analysed is highlighted in blue), the main topographic features mentioned in the text, and the location of the tide gauge and bottom pressure measurement sites used for validation of the tidal constituents. Red circles indicate the tide gauges used in the analysis of the cross-strait variability.

Figure 2. Radargram of the RA-2 radar waveform power for a rejected (Fig. 2.a) and a valid (Fig. 2.b) cycle. The cycle-by-cycle AT_SLA for valid cycles is shown in Fig. 2.c.

Figure 3. AT_SLA (5-elements running mean applied) for valid cycles using the global DT15MSS (Fig. 3.a) and the local AT_MSS (Fig. 3.b). The green line gives the bathymetry profile.

Figure 4. Mean Dynamic Topography (in cm) in the Strait of Gibraltar from the global model MDT_DTU15 (5.a) and the local model MDT_UCA2D (5.b).

Figure 5. Cycle-by-cycle AT_ADT for valid cycles (Fig. 5.a). AT_ADT for cycle 51 (Fig. 5.b) and 50 (Fig. 5.c). The average of AT_ADT over all valid cycles is also shown in Fig. 5.b and 6.c (red line).

Figure 6. Correlation coefficient between the calculated zonal component (û) and the sea level gradient between the two tide gauge stations (Ceuta and Tarifa) for increasing time intervals (Nh).

Figure 7. Cross-strait sea level differences between the African and Spanish coasts as a function of the mean zonal û component of the wind. Fig. 7.a gives the comparison using altimeter data and Fig. 7.b in-situ data. The numbers indicate the cycle number of the satellite pass.